Available online at www.sciencedirect.com
SCIENCE DIRECT
Thin Solid Films 488 (2005) 211 – 216
thin solid films
www.elsevier.com/locate/tsf

The nitrogen doping effect on the properties of Ge–In–Sb–Te phase-change recording media investigated by blue-light laser

Tung-Ti Yeh[a], T.-E. Hsieh[a,*], Han-Ping D. Shieh[b]

[a]Department of Materials Science and Engineering, National Chiao-Tung University, 1001, Ta-Hsueh Rd., Hsinchu 30049, Taiwan, ROC
[b]Department of Photonics and Institute of Electro-Optical Engineering, National Chiao-Tung University, 1001, Ta-Hsueh Rd., Hsinchu 30010, Taiwan, ROC

Received 9 January 2004; received in revised form 7 September 2004; accepted in revised form 15 April 2005
Available online 23 May 2005

Abstract

This work investigates the thermal, optical and recrystallization properties as well as the microstructure of nitrogen-doped Ge–In–Sb–Te (GIST) phase-change material when irradiated by blue-light laser. The experimental results showed that nitrogen doping at the condition of N_2/Ar sputtering gas flow ratio equals to 3% might enhance the recrystallization speed of GIST recording layer up to 1.5 times. However, the disk failed when too much nitrogen (N_2/Ar ≥ 5.0%) was introduced. The data obtained by differential scanning calorimetry, X-ray diffraction and ellipsometry revealed changes of thermal and optical properties due to the nitrogen doping in GIST. When appropriate amount of nitrogen was added, the activation energy (E_a) of amorphous–crystalline phase transition of GIST decreased and the optical constants of amorphous and crystalline phases (except the k value of amorphous phase) gradually reduced with the increase of wavelength in the range of 600–750 nm. Modulation simulation based on the reflectively of doped GIST layers obtained from static test indicated that appropriate nitrogen doping benefited the signal characteristics of optical disks. Transmission electron microscopy observed numerous tiny precipitates uniformly distributed in the doped GIST layers. These were believed to be nitride particles generated by nitrogen doping that might offer the preferential sites for amorphous–crystalline phase transition so that the recrystallization speed was accelerated.

PACS: TSF-04
Keywords: Ge–In–Sb–Te phase-change recording media; Nitrogen doping; Recrystallization speed; Microstructure

1. Introduction

The development of optical disks using phase-change materials as the recording media always pursues large storage capacity and high data transfer rate. In 1999, Sony and Philips announced the format of "next generation" optical disk system for digital video recording (DVR) [1]. The second version of DVR used a blue-light laser diode (λ=405 nm) and high numerical aperture (NA=0.85) allowing a disk capacity of 22.5 GB so that the blue-light laser recording is emphasized on optical data storage. Currently the eutectic Sb–Te system, or called the fast-growth phase-change material, has drawn a lot of attentions since it possesses excellent signal properties and high recrystallization speed when employing short wavelength laser and high NA lens. The quaternary Ge–In–Sb–Te (GIST) alloy based on the Sb–Te eutectic system has been used as the recording layer in the phase-change optical disks such as compact disk-rewritable [2], digital versatile disk-rewritable [2,3], and DVR disk [4,5], etc.

Recently, nitrogen doping has been adopted to improve the performance of phase-change optical disks [6–8]. Nitrogen atoms in phase-change material might exist as interstitials or form the nitrides by interacting with other alloy elements. It would cause the microstructure and phase constitution change of phase-change material and affect the direct overwriting [6], optical [7], thermal and signal properties [6–8] of recording media. Nevertheless, most of the studies related to nitrogen doping focused on the stoichiometric materials such as $Ge_2Sb_2Te_5$, $Ge_1Sb_4Te_7$ and $Ge_1Sb_2Te_4$, etc., and the eutectic Sb–Te system is yet to be

* Corresponding author. Tel.: +886 3 5712121 55306.
E-mail address: tehsieh@cc.nctu.edu.tw (T.-E. Hsieh).

0040-6090/$ - see front matter © 2005 Elsevier B.V. All rights reserved.
doi:10.1016/j.tsf.2005.04.062

Table 1
Sample preparation conditions

N_2/Ar ratio[a]	Target material	Sputtering pressure (Pa)	Sputtering power (W)
NA	$ZnS-SiO_2$ (80:20)		250 (RF)
NA	Al–Cr (99:1)		400 (DC)
0%			
0.5%		0.5	
1.0%	GeInSbTe[b]		50 (RF)
3.0%			
5.0%			
10.0%			

[a] Ar flow was fixed at 10 sccm.
[b] Ge:In:Sb:Te=4.5:4:65.95:25.55 (in wt.%).

explored. In this work, we dope nitrogen in the eutectic GIST recording layer of the optical disks and investigate their effects on recrystallization speed using blue-light laser. Differential scanning calorimetry (DSC), X-ray diffraction (XRD), ellipsometry and Transmission electron microscopy (TEM) were adopted to examine the changes of thermal, optical properties, and microstructures induced by nitrogen doping and the effects on the recrystallization speed of phase-change recording material are discussed.

2. Experimental details

The samples for static testing were prepared using a SFI (Surface Interface Corp.) sputtering system with background pressure better than 1.33×10^{-4} Pa. The multilayer structure was deposited on 0.6-mm-thick polycarbonate (PC) substrate in the sequence of $ZnS-SiO_2$ (55 nm)/GIST-$(N)_x$ (16 nm)/$ZnS-SiO_2$ (11 nm)/Al–Cr (133 nm). During the deposition of recording layer, the N_2/Ar flow rate was adjusted at values of 0%, 0.5%, 1.0%, 3.0%, 5.0%, and 10.0% in order to obtain the doped specimens with various nitrogen contents. The sputtering conditions are listed in Table 1 and each of samples is characterized by the N_2/Ar ratio depicted in Table 1. After initialized by the condition of 1000 mW laser power, 50 μm per revolution and 2.0 m/s linear velocity, the disks were sent to a static tester (MEDIA TEST-1) that monitors the change of reflectance for phase-change media during the writing and erasing processes. The MEDIA TEST-1 uses two different laser sources (λ=422 and 389 nm) in order to separate the effects of writing/erasing and reading and to independently control the write/erase and read powers. The recorded mark images could be observed directly by using the attached optical microscope with a video camera for image capture.

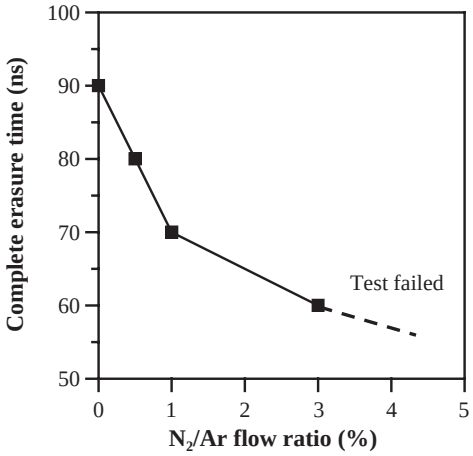

Fig. 2. Complete erasure time (CET) versus the doping N_2/Ar flow ratios.

The recrystallization temperatures of the amorphous GIST-$(N)_x$ films at different heating rates (5, 10, 20, 40 and 80 °C/min) were measured using a DSC (Dupont 2000 Series) and then fitted into the Kissinger plot to calculate the activation energy for recrystallization. The 1-μm-thick GIST-$(N)_x$ samples were deposited on 7059 optical glass and recrystallized by annealing at 300 °C for 1 h. The XRD analysis was carried out in a Siemens D-5000 diffractometer with Cu K_α radiation (λ=0.1542 nm). The XRD data were collected in the diffraction angle (2θ) ranging from 20° to 80° with scanning rate of 2°/min. The 16-nm-thick GIST-$(N)_x$ samples were also deposited on a (100) Si single-crystal wafer for optical constants (n and k) characterization using an ellipsometer (J.A. Woollam, M-44) with an visible light source (λ=405 to 750 nm).

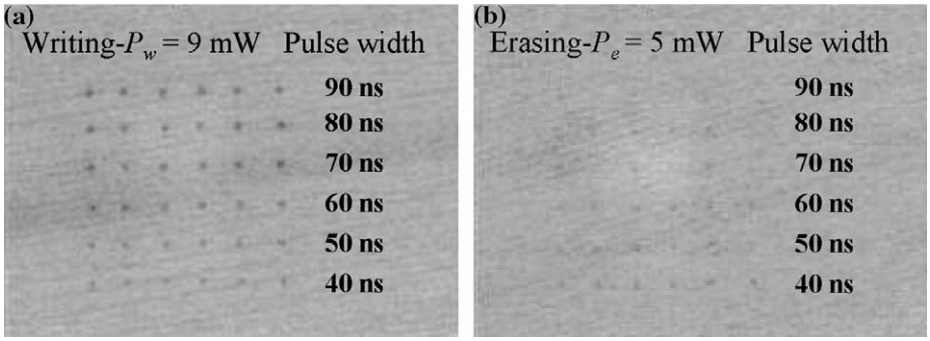

Fig. 1. The optical microscope images of (a) written and (b) erased arrays of 0% sample observed by static tester. The pulse width for each row of marks is specified at the right-handed side of the images.

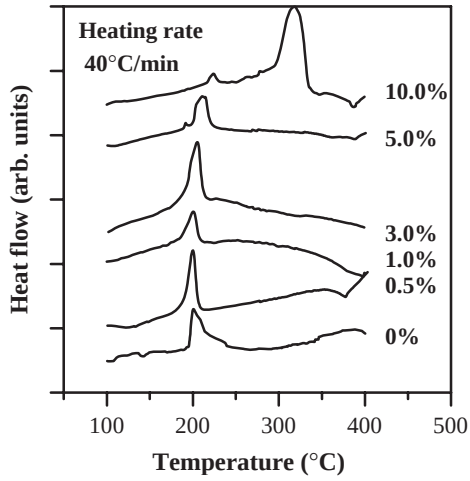

Fig. 3. The DSC profiles of GIST samples subject to various amount of nitrogen doping (heating rate=40 °C/min).

The method reported by Nobukuni et al. and Chen et al. [9,10] was adopted to prepare the plan-view TEM (PTEM) specimens. After removing the PC substrate, the disk sample was cut into small pieces using a scissor. A 3M tape was applied on the disk to peel off the Al–Cr reflection layer. After dissolution of the PC substrate by CH_2Cl_2 solution, the specimen was mounted on the copper mesh and transferred to TEM (Philips, TECNAI 20) for microstructure observation.

3. Results and discussion

At the beginning of static test, the appropriate writing and erasing powers (5 and 9 mW) were identified by using the method of optical microscopic observation. The samples were written and erased at various pulse widths (40 to 90 ns) at predetermined 5 and 9 mW. The written and erased mark arrays of 0% sample shown in Fig. 1 could be observed directly by the optical microscope attached to the static tester. Not only mark arrays but also the changes of reflectance were recorded in order to determine the minimum write and erase pulse widths for subsequent writing and erasing processes. The complete erasure time (CET) is defined as the minimum duration of the erase pulse for complete crystallization of a written amorphous mark in a crystalline background [11]. As shown in Fig. 2, the CET of various samples was measured and it was found that the static test failed when too much nitrogen ($N_2/Ar \geq 5.0\%$) was doped in the recording layer. Numerous void-like defects likely resulted from reactive sputtering etching of N_2 were observed on the sample surfaces and caused the test failure. The static test indicated that the CET decreased with the increase of nitrogen content in GIST layer in the doping range of $N_2/Ar \leq 3.0\%$. The shorter the CET, the higher the

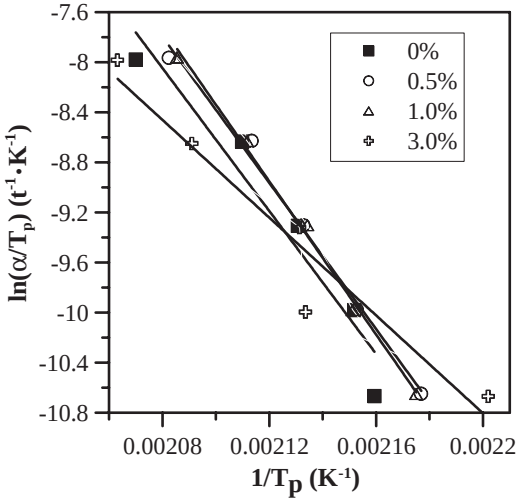

Fig. 4. The Kissinger plot of 0%, 0.5%, 1.0%, and 3.0% samples.

Table 2
Calculated activation energy for 0%, 0.5%, 1.0%, and 3.0% samples according to Kissinger plot shown in Fig. 4

Sample	0%	0.5%	1.0%	3.0%
Activation energy (eV)	2.462	2.521	2.642	1.686

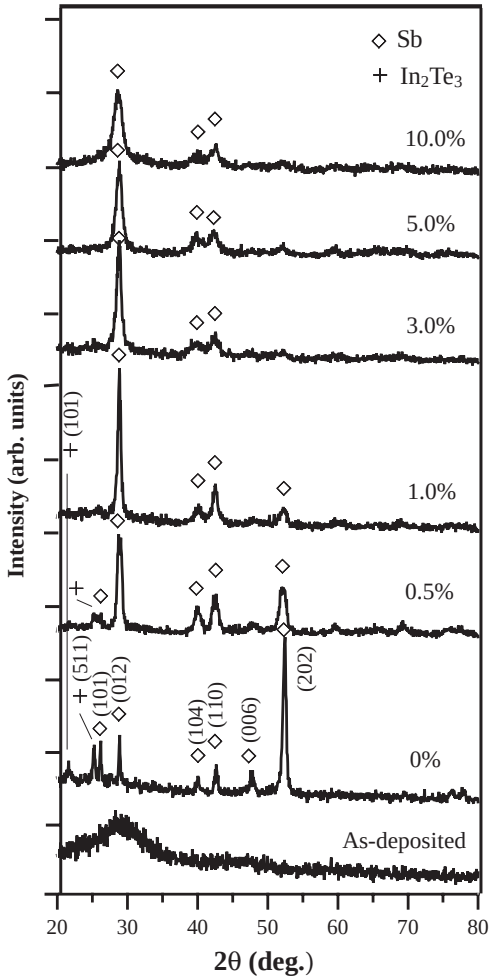

Fig. 5. The XRD patterns of undoped and doped GIST samples annealed at 300 °C for 1 h.

recrystallization speed since the CET is inversely proportional to the recrystallization speed during erasing. From the values of CET depicted in Fig. 2, it is concluded that the recrystallization speed of 3.0% sample was about 1.5 times higher than that of sample free of nitrogen. Hence appropriate amount of nitrogen doping was able to increase the recrystallization speed of GIST phase-change optical disks. Higher recrystallization speed should be possible in the samples doped at $N_2/Ar \geq 5\%$, however, this could not be justified from static test since the measurement of CET was failed due to imperfections in sample.

Fig. 3 shows the DSC profiles of GIST samples subjected to 40 °C/min heating rate. It can be seen that only one exothermic peak appears for the specimens doped at the N_2/Ar flow ratio $\leq 3.0\%$, and the recrystallization temperatures of 0%, 0.5%, 1.0%, and 3.0% samples are almost the same. The second exothermic peak appears when too much nitrogen ($N_2/Ar = 10.0\%$) was introduced in GIST layers, as illustrated by the DSC profile corresponding to N_2/Ar = 10.0% in Fig. 3. The second exothermic peak might associate with the formation of new compound phases resulted from high percentage of nitrogen doping.

Five different recrystallization temperatures at different heating rates (5, 10, 20, 40 and 80 °C/min) were fitted into the Kissinger equation [12] given by Eq. (1) to calculate the activation energy for crystallization:

$$\ln\left(\frac{\alpha}{T_P^2}\right) = -\left(\frac{E_a}{R}\right)T_P^{-1} + C. \quad (1)$$

In Eq. (1), α is the heating rate, T_P is the recrystallization temperature, E_a is the activation energy for phase transition, R is the gas constant and C is a constant. The plots of $\ln(\frac{\alpha}{T_P^2})$ *versus* $\frac{1}{T_P}$ for 0%, 0.5%, 1.0% and 3.0% samples yielded the straight lines as shown in Fig. 4 and the activation energy for amorphous-to-crystalline transition can be calculated. Table 2 shows the calculated E_a for 0%, 0.5%, 1.0%, and 3.0% samples. It can be seen that E_a values were almost the same when doping flow ratio was below 1.0% and then rapidly decreases when the $N_2/Ar = 3.0\%$. Decrease of activation energy for phase transition evidenced the increase of recrystalliztion speed deduced from the measurement of CET.

Fig. 5 shows the XRD patterns of GIST samples subject to various amounts of nitrogen doping. The phase constitution of all the samples, regardless of the amount of nitrogen doping, could be viewed as a mixture of Sb and In_2Te_3. It can be seen that the nitrogen doping performed in this work did not cause obvious position change of

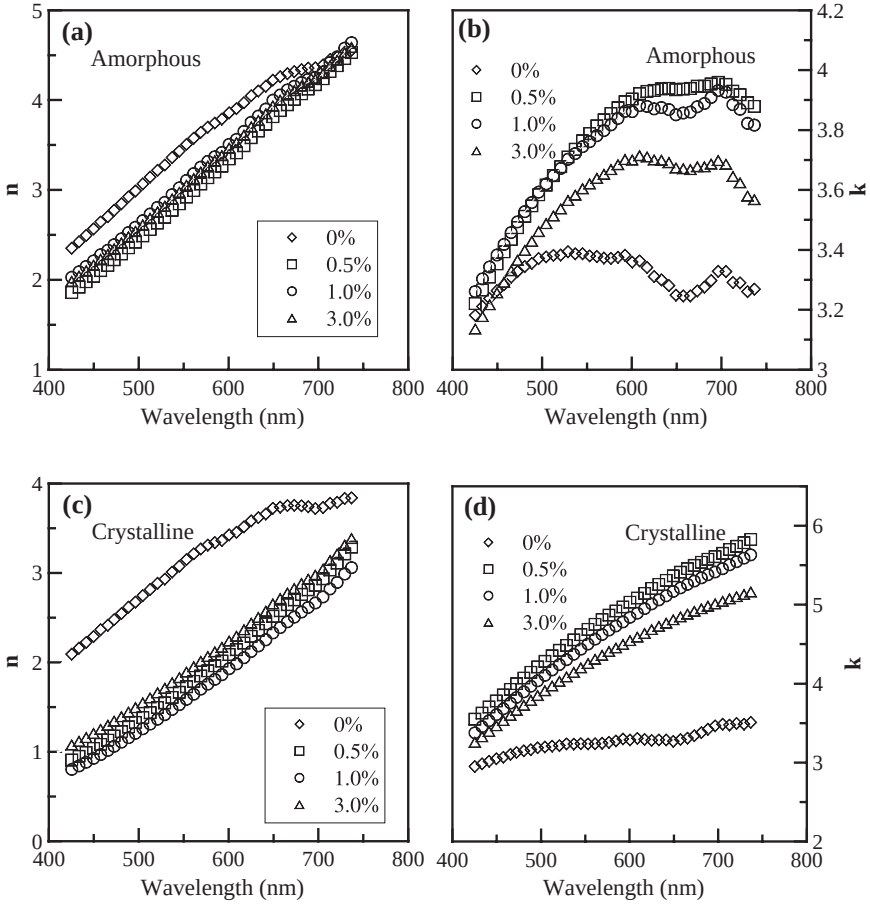

Fig. 6. The optical constants (n and k) versus laser wavelength for 0%, 0.5%, 1.0%, and 3.0% samples. The plots in (a) and (b) respectively show the variation of n and k for amorphous phase while the plots in (c) and (d) respectively show the variation of n and k for crystalline phase.

characteristic peaks. However, it did cause the change of peak height and the width of peaks also increased with the increase of N_2/Ar flow ratio, which is similar to the work reported by Jeong et al. [13]. The results of XRD indicated that a certain portion of nitrogen should occupy the interstitial sites of GIST lattice. When the number of interstitial nitrogen atoms increased, the lattice distortion became severer hence we observed the broadness of XRD characteristic peaks increased with the increase amount of nitrogen doping, as shown in Fig. 5. Though previous DSC characterization indicated the formation of new nitride phases, they might be in amorphous state that showing no characteristic peak in XRD pattern to reveal their existence.

Fig. 6 presents the wavelength dependence of optical constants (refractive constant n and extinction coefficient k) of GIST layers in the range of 0–3.0% N_2/Ar doping ratios. It can be seen that, regardless of the crystallinity of GIST layer, nitrogen doping did change the optical constants of recording material. Fig. 6 shows that n and k values of the amorphous and crystalline phases gradually increase with the increase of wavelength ranging from 600 to 750 nm, except the k value of amorphous phase. We utilized the reflectively obtained from static test to calculate the modulation of 0%, 0.5%, 1.0% and 3.0% disk samples and the modulation of optical disks was determined by using the formula below:

$$\text{modulation } (\%) = \frac{R_c - R_a}{R_c + R_a} \times 100\% \qquad (2)$$

in which R_c=the total reflectivity of optical disk when the recording material is in crystalline state and R_a=the total reflectivity of optical disk when the recording material is in amorphous state. As shown in Table 3, appropriate nitrogen doping might raise the modulation of optical disk such as 3% disk sample. This evidences that the appropriate nitrogen doping in GIST recording layers would benefit the signal characteristics of optical disks.

Fig. 7 shows the TEM micrographs of 0%, 3.0%, and 5.0% disk samples immediately after initialization. The lamellar-like structure commonly seen in the eutectic recording alloys was observed in these samples. In addition to the higher degree of structure irregularity, we observed tiny precipitates uniformly distributed in 3.0% sample as shown in Fig. 7(b). The tiny precipitates were believed to be the nitride phases generated by nitrogen doping. These precipitates might offer the preferential sites for amorphous–crystalline phase transition so as to accelerate the recrystallization speed of GIST recording layer. Comparison of Fig. 7(b) and (c) shows that the density and sizes of the precipitates increase with the increase of N_2 content. Further increase the number of tiny precipitates might benefit the recrystallization speed of GIST layer, however, many void-like defects resulted from the reactive sputtering etching of N_2 were observed on sample surface and failed the static test when $N_2/Ar \geq 5\%$.

Table 3
Simulated modulation of optical disks at various content

Sample	0%	0.5%	1.0%	3.0%
Modulation (%)	7.85	8.95	7.40	10.28

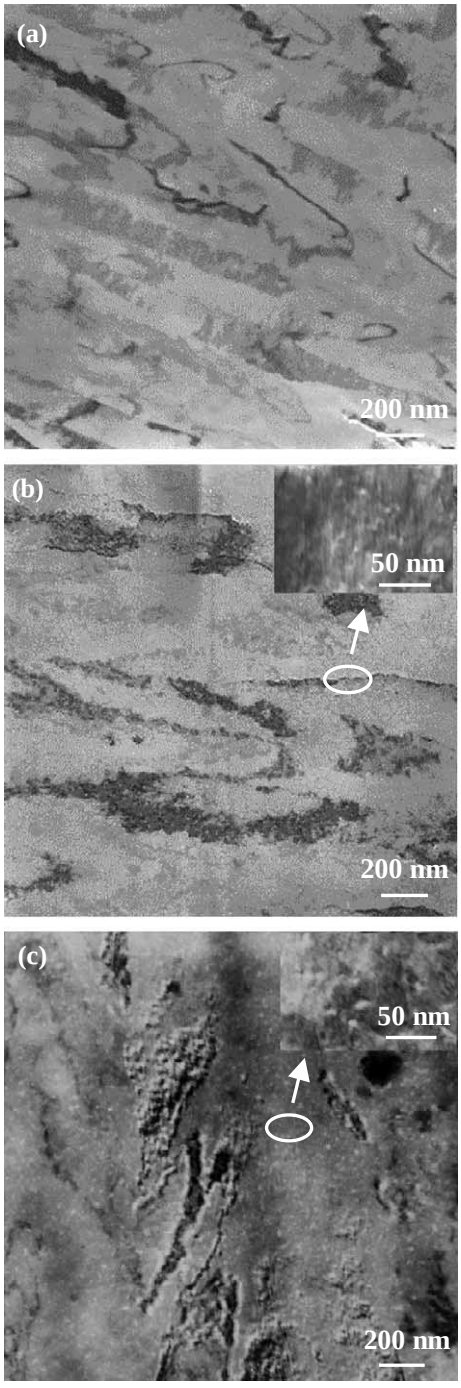

Fig. 7. The microstructure of (a) 0%, (b) 3.0%, and (c) 5.0% disk samples after initialization. Local magnifications of (b) and (c) are respectively attached at the upper right-handed corner of micrographs.

4. Model of recrystallization

The eutectic GIST alloy is termed as the fast-growth material since its recrystallization is initiated from the

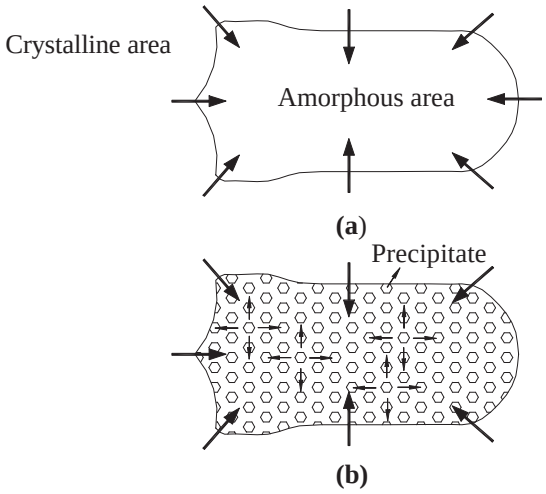

Fig. 8. Schematic illustration of the recrystallization model for (a) undoped and (b) nitrogen-doped samples. In (a), phase transition mostly occurs at the amorphous–crystalline phase boundary while in (b), the phase transition might also initiate from the tiny precipitates inside the mark.

crystalline–amorphous interface and the amorphous mark shrinks as the grain growth propagates toward the center of the mark [14–17], as illustrated in Fig. 8(a). The velocity of grain growth derived from the net jump frequency of atoms across the amorphous–crystallization interface can be expressed as [15]

$$V(T) = V_0 e^{\frac{E_a}{RAT}}\left(1 - e^{\frac{\Delta g^{ac}}{RT}}\right), \quad (3)$$

where V_0 is a pre-exponential factor, E_a is the activation energy of amorphous-to-crystalline phase transition, Δg^{ac} is the free energy difference between an atom in the amorphous state and in the crystalline state, R is the gas constant and ΔT is the temperature difference between the interface temperature and the glass transition temperature of GIST. From Eq. (3), it is known that low E_a value benefited amorphous-to-crystalline phase transition. According to the recrystallization model shown in Fig. 8(b), nitrogen doping might generate numerous nanometer-scale precipitates uniformly distributed in the GIST recording layer. In addition to the amorphous–crystalline edge of marks, they were also the preferential sites for amorphous–crystalline transition of recording media. The tiny precipitates not only induce the heterogeneous nucleation, they also shorten the distance of grain growth required to complete the transition. The value of E_a was then decreases accordingly and the speed of amorphous–crystalline transition is promoted.

5. Conclusions

We demonstrated that nitrogen doping is a promising method to enhance the recrystallization speed of GIST phase-change recording materials irradiated by blue-light laser. According to our static test, the recrystallization speed of GIST recording layer was increased about 1.5 times when the optical disks were doped at the condition of N_2/Ar=3.0%. The data of DSC revealed that there was no obvious change of recrystallization temperatures of GIST materials when $N_2/Ar \leq 5.0\%$. Too much nitrogen (N_2/Ar=10.0%) doping did not benefit the data recording since it would result too many void-like defects on sample surface and change the phase constitution of GIST layers, as evidenced by static test and DSC analyses, respectively. Optical property characterization and modulation simulation indicated that appropriate nitrogen doping in GIST recording layer benefits the signal characteristics of optical disks. The TEM observation revealed that the nitrogen doping products tiny precipitates uniformly distributed in the recording layer. These tiny precipitates provided numerous preferential sites for heterogeneous amorphous–crystalline phase transition so as to promote the recrystallization speed of GIST materials.

Acknowledgement

This work was supported by the Ministry of Education of the Republic of China with the Academic Center of Excellence in “Photonics Science and Technology for Tera Era” under contract No. 89-E-FA06-1-4 as well as the National Science Council of the Republic of China under contract No. NSC91-2216-E-009-031.

References

[1] T. Schep, B. Stek, R.V. Woudenberg, M. Blum, S. Kobayashi, T. Narahara, T. Yamagami, H. Ogawa, Jpn. J. Appl. Phys. 40 (2001) 1813.
[2] B. Bechevet, R. Paviet, R. Perrier, J.M. Bruneau, U.S. Patent NO. 0119278, 29 Aug. 2002.
[3] T. Abiko, A. Konishi, T. Kanesaka, H. Shimomuki, U.S. Patent NO. 00036528, 1 Nov. 2001.
[4] H. Inoue, H. Hirata, T. Kato, H. Shingai, H. Utsunomiya, Jpn. J. Appl. Phys. 40 (2001) 1641.
[5] T. Kato, H. Hirata, T. Komaki, H. Inoue, H. Shingai, N. Hayashida, H. Utsunomiya, Jpn. J. Appl. Phys. 41 (2002) 1664.
[6] R. Kojima, S. Okabayashi, T. Kashihara, K. Horai, T. Matsunaga, E. Ohno, N. Yamada, T. Ohta, Jpn. J. Appl. Phys. 37 (1998) 2098.
[7] S.Y. Kim, S.J. Kim, H. Seo, M.R. Kim, Jpn. J. Appl. Phys. 38 (1999) 1713.
[8] H. Seo, T.H. Jeong, J.W. Park, C. Yeon, S.J. Kim, S.Y. Kim, Jpn. J. Appl. Phys. 39 (2000) 745.
[9] N. Nobukuni, M. Takashima, T. Ohno, M. Horie, J. Appl. Phys. 78 (1995) 6980.
[10] H.W. Chen, T.E. Hsieh, J.R. Liu, H.P.D. Shieh, Jpn. J. Appl. Phys. 38 (1999) 1691.
[11] G.F. Zhou, B.A.J. Jacobs, Jpn. J. Appl. Phys. 38 (1999) 1625.
[12] H.E. Kissinger, Anal. Chem. 29 (1957) 1702.
[13] T.H. Jeong, M.R. Kim, H. Seo, J.W. Park, C. Yeon, J. Appl. Phys. 39 (2000) 2775.
[14] R.E. Reed-Hill, R. Abbaschin, Physical Metallurgy Principles, 2nd ed., Van Nostrand, 1991.
[15] D.A. Porter, K.E. Easterling, Phase Transformations in Metals and Alloys, Van Nostrand, Reinhold, 1981.
[16] L.H. Chou, Y.Y. Chang, Jpn. J. Appl. Phys. 40 (2001) 1272.
[17] E.R. Meinders, H.J. Borg, M.H.R. Lankhorst, J. Hellmig, A.V. Mijiritskii, J. Appl. Phys. 91 (2002) 9794.